

SHORT-PERIOD *P*- AND *S*-WAVE RADIATION FROM LARGE EARTHQUAKES: IMPLICATIONS FOR SPECTRAL SCALING RELATIONS

BY DAVID M. BOORE

ABSTRACT

Recent measurements of peak *P*-wave amplitudes on World Wide Standardized Seismographic Network short-period instruments by Houston and Kanamori (1986) provided the opportunity to investigate source radiation from great earthquakes at higher frequencies than have previously been available. The dependence on moment magnitude (*M*) of the amplitude measurements (*A*) and the dominant period (*T*) in the *P*-wave seismograms are compared to predictions from several source-scaling relations. For all of the relations, the radiated energy was assumed to be randomly distributed over a duration proportional to the inverse corner frequency. An ω -square source-scaling relation with a constant stress parameter of 50 bars gives a good fit to both observed quantities (*A* and *T*) for earthquakes up to *M* 9.5. This model, with the same stress parameter, also fits peak acceleration and peak velocity data for earthquakes with moment magnitude as low as 0.5. Predictions using the source spectra derived by Gusev (1983), which are representative of several published relations featuring regions of reduced spectral decay after an initial ω^{-2} attenuation beyond the corner frequency, do not fit the various high-frequency observations quite as well as do those using the ω -square model, although the differences between the predicted motions are generally within a factor of 2 to 3. Although the ω -square model successfully predicts a wide variety of time-domain measures over an extraordinary magnitude range, it fails to fit the M_s , *M* correlation for large earthquakes; Gusev's spectral scaling relation, on the other hand, fits this correlation, but was constrained in advance to do so. This failure of the ω -square model is of little practical concern, occurring as it does at periods longer than those of usual engineering importance. An ω -cube model fails completely to explain the seismic moment dependence of the observations.

INTRODUCTION

Although crucial for many engineering designs of critical structures, knowledge of the high-frequency radiation from large and great earthquakes is hampered by the lack of suitable recordings of such events at distances for which significant damage can occur (within 100 to 200 km). Because of the long recurrence times of large earthquakes and their generally inaccessible locations, it may be years before such records are collected. Lacking records, seismic design criteria are often based on extrapolations from the existing data base—extrapolations that can be guided by theoretical predictions based on seismic scaling laws. One such scaling law that has proven to give good predictions of strong ground motion at close distances is the stochastic, ω -square, constant-stress-parameter model (Hanks, 1979; McGuire and Hanks, 1980; Hanks and McGuire, 1981; Boore, 1983; McGuire *et al.*, 1984; Atkinson, 1984). Does this model also work for great earthquakes? Are other scaling laws comparable or better? To answer these questions, it is natural to turn to short-period recordings of great earthquakes at teleseismic distances.

Although recent improvements in digital seismometry have made possible the

direct estimation of body-wave spectra at short periods (e.g., Houston and Kanamori, 1986), there are few large and great earthquakes for which adequate records are available. Because of this limitation, most of the existing scaling laws are based in one way or another on relations between various magnitude measures (usually m_b and M_S) and seismic moment. The teleseismic magnitude most directly related to the frequencies of engineering interest is the body-wave magnitude m_b . There are two problems connected with using published m_b 's to investigate scaling laws: the first is that the standard m_b published by the National Earthquake Information Service (NEIS) or the International Seismological Centre (ISC) is largely determined from amplitudes in the first several cycles of motion. The resulting m_b for large earthquakes may not contain any information about the overall radiation of short-period waves. The second problem is the technical one of relating a peak motion in the time domain to a spectral amplitude. As pointed out by Hanks (1979), if the duration of the body-wave phase on the seismogram is controlled by the source duration, then the peak time-domain amplitude is not simply proportional to the spectral amplitude at the predominant frequency of the seismogram. This has been recognized and accounted for by some authors of scaling laws (e.g., Aki, 1967; Gusev, 1983) but apparently not by others (Geller, 1976; Nuttli, 1983a,b, 1985). The problem of m_b not being representative of the overall source radiation can be overcome by using measurements of the maximum amplitude of the P wave on short-period recorders (Koyama and Zheng, 1985; Houston and Kanamori, 1986). I have resolved the problem of relating time- and frequency-domain amplitudes by using random vibration theory (with time-domain simulation as a check) for predictions of the peak time-domain seismograph response for various spectral scaling relations.

DATA

Houston and Kanamori (1986) studied the short-period radiation of large earthquakes using teleseismic recordings of 19 moderate to great earthquakes. Although of less engineering significance than S waves, Houston and Kanamori chose to study P waves because they are little contaminated by later phases and even for great earthquakes are often recorded at teleseismic distances without saturating on conventional analog short-period instruments. For all but one of the 19 events studied, Houston and Kanamori used 8 to 27 records from WWSSN short-period stations at distances of 30° to 100° . For the 1960 Chilean event, records from short-period Benioff, Wood-Anderson, Milne-Shaw, and short-period Willmore seismographs were used. The measurements of maximum amplitude in the P -wave train were converted into an effective body-wave magnitude, \hat{m}_b , using the same formula from which conventional m_b magnitudes are derived. A plot of \hat{m}_b as a function of moment magnitude, M (Kanamori, 1977; Hanks and Kanamori, 1979), is given in Figure 1. For reference, a plot of m_b versus M for earthquakes with focal depths less than 70 km has also been included in part b of the figure. The m_b values were taken from the *International Seismological Centre Bulletin*, if available, and the Preliminary Determination of Epicenters, National Earthquake Information Service (NEIS), if not. The moments were compiled from five sources, as given in the legend. Approximate bounding lines have been drawn on the $m_b - M$ plot, and these have been included in the \hat{m}_b plot (part a of the figure). The first point to make is that, contrary to widespread expectations, on-scale recordings of short-period radiation from great earthquakes are readily available (although not easily

analyzable). Besides providing direct information about the radiation, these data give important constraints for modeling great earthquakes. The second, and most important, point is that \hat{m}_b shows no indication of saturation with earthquake size, as is commonly ascribed to m_b . The difference in m_b and \hat{m}_b is that in practice many of the amplitudes used in determining the former are measured from only the first few cycles of the P -wave motion. Not being a true measure of the maximum P -wave motion, m_b gives a misleading impression of the scaling of P -wave motion with source size. Current recommendations of the International Association of Seismology and Physics of the Earth's Interior for measuring peak amplitudes (and current in-house procedures of the NEIS) will help alleviate this for all but the largest earthquakes (Willmore, 1979; B. W. Presgrave, oral communication, 1984).

The period (T) measured by Houston and Kanamori is their estimate of the dominant period in the vicinity of the peak motion; it is measured from adjacent peaks on the seismogram. On the other hand, the random vibration theory used to

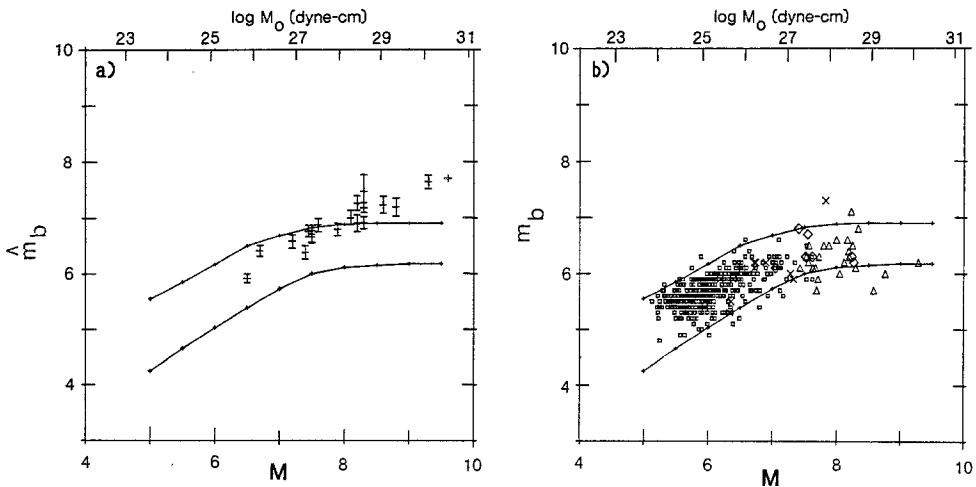


FIG. 1. Dependence of short-period P -wave magnitude on moment magnitude (M). (a) \hat{m}_b versus M . Errors bars are 95 per cent confidence limits. Data from Houston and Kanamori (1986) and H. Houston (written communication, 1984). Lines are approximate bounds of m_b , M relation, fit to the data by eye. (b) m_b versus M taken from several sources, with same bounding lines as in (a). Source depths less than 70 km. (Squares) Dziewonski and Woodhouse (1983), Dziewonski *et al.* (1983); (X) Geller (1976); (diamonds) Silver and Jordan (1983); (triangles) Furumoto and Nakanishi (1983).

compute theoretical estimates of T predicts the period that would be measured from the frequency of crossings of the seismogram's zero line. These two estimates of period can be different. Measurements on a subset of the seismograms used by Houston and Kanamori (corresponding to 22 of the best recordings from 5 of the earthquakes) indicated little relation between the two period measures (Figure 2). On average, the periods determined from crossings of the baseline are 0.4 sec lower than those measured from the distance between peaks, and there is less scatter in the former period measure. Because it is more closely related to the quantity predicted by theory, the average zero-crossing period (1.4 sec) is used as the observational quantity against which the predicted values will be compared. For the larger earthquakes, little or no dependence of period on moment magnitude was observed by Houston and Kanamori or predicted by theory.

The formula from which magnitude is defined includes period explicitly in the

divisor of the observed amplitude and implicitly in the correction for instrument response. Because of the difference in the period measure used by Houston and Kanamori and that computed with the simulation method, I decided that it would be more consistent to compare the theoretical predictions with the observed seismogram amplitudes, before they were reduced to magnitudes. To do this, measurements provided by H. Houston (written communication, 1984) were normalized to

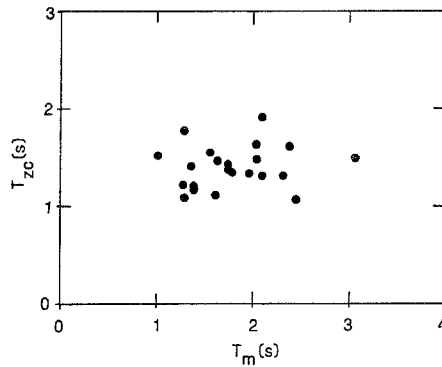


FIG. 2. Periods measured by H. Houston from peaks adjacent to maximum (T_m) and by D. Boore from zero crossing (T_{zc}), for a subset of earthquake/station pairs used by Houston and Kanamori (1986).

TABLE 1
WWSSN SEISMOGRAM AMPLITUDES REDUCED TO 70° and Gain of 10,000

Earthquake*	$\log 10^4 A/G^\dagger$	95% Confidence Limits	No. of Stations
1	0.49	± 0.11	19
2	0.15	± 0.17	17
3	0.11	± 0.13	20
4	0.30	± 0.30	8
5	0.10	± 0.11	27
6	-0.21	± 0.13	9
7	-0.20	± 0.14	16
8	0.05	± 0.10	16
9	-0.17	± 0.15	17
10	-0.31	± 0.13	20
11	-0.38	± 0.15	17
12	-0.43	± 0.16	18
13	-0.31	± 0.09	21
14	-0.42	± 0.12	17
15	-0.56	± 0.12	17
16	-0.69	± 0.12	22
17	-0.59	± 0.09	26
18	-1.17	± 0.09	19

* Corresponds to Houston and Kanamori (1986) numbering.

† Units of A are in centimeters.

a gain of 10,000, and the logarithms of the normalized amplitudes were reduced to a distance of 70°. The resulting measure of seismogram amplitude will be referred to as “ A ” from here on. The reduction to a common distance used the standard Gutenberg-Richter correction function (e.g., Richter, 1958, p. 688). The measured periods showed no dependence on distance, thus justifying the use of the correction function for the log of the seismogram amplitudes rather than the log of amplitudes divided by period. The values of A are given in Table 1.

SIMULATION OF *A* AND *T*: METHOD

The *A*, *T* data should put some constraints on the short-period seismic radiation. To study this quantitatively, I constructed theoretical *A* and *T* for several spectral scaling relations. The procedure for doing this was straightforward: the source spectrum for an event of given moment magnitude was corrected for geometric spreading and anelastic attenuation and then multiplied by the WWSSN short-period instrument response. Random vibration theory (e.g., Boore, 1983, p. 1884), which uses various spectral moments of the resulting instrumental spectrum, provided estimates of the characteristic period and the peak amplitude. This procedure differed in several essential ways from that used in many scaling studies: the assumption that \hat{m}_b (or, equivalently, the peak amplitude of the seismogram) is proportional to the log of the spectral amplitude at a particular frequency was avoided, and absolute values of *A* were predicted (rather than relative values that are tied to a particular \hat{m}_b , *M* pair by an empirically determined additive constant).

The emphasis in this research was on testing several well-known models for their consistency with the average trends defined by the observations; detailed predictions of observed quantities for particular events were not attempted, nor were attempts made to optimize the fit of any model to all the data. Because observations of *A* and *T* were made from various azimuths for any one event and for events with various focal depths (down to 70 km) and many varieties of tectonic regimes, a simple point source in a uniform medium was chosen as the basis of the theoretical calculations; source directivity is generally negligible for teleseismic *P* waves and was ignored. With these assumptions, the equation used to estimate the record spectrum *R*(*f*) is

$$R(f) = C \frac{g(\Delta)}{r} S(f)D(f)Z(f)I(f), \quad (1)$$

where the symbols *C*, *S*, *D*, *Z*, and *I* stand for a scaling factor, the spectrum of moment-rate, a diminution factor, an amplification factor, and the instrument response, respectively. Only *S* depends on the seismic moment; it is discussed in detail in a later section. *g*(Δ) is a geometrical spreading factor, and *r* is the radius of the Earth (for predictions at teleseismic distances). *C* is given by

$$C = \frac{R_{\Theta\Phi} \cdot F}{4\pi\rho_s c_s^3}, \quad (2)$$

where $R_{\Theta\Phi}$ is a radiation coefficient, *F* is the free surface amplification, and ρ_s and c_s are the density and the wave velocity in the vicinity of the source. Values for some of the constants used in this paper are given in Table 2.

In previous analyses (e.g., Boore, 1983; Hanks and Boore, 1984), no effort was made to account for the amplification of waves as they travel upward through rocks whose velocities generally decrease as the Earth's surface is approached. For the periods contained in teleseismic recordings of *P* waves and WWSSN short-period instruments sited on rock, this amplification is not great. For close-in, rock recordings of *S* waves, however, the amplification can be greater than a factor of 2, especially as frequencies increase beyond 1 Hz. This is true even in the absence of strong impedance contrasts. For the sake of completeness in describing the model, an amplification correction is discussed here although its major importance is not

encountered until the later section dealing with strong-motion simulations. A first-order way of accounting for the amplification effect is to use energy conservation in a ray tube passing through media of slowly changing velocity. Although such a correction is included in the equation from which $g(\Delta)$ is derived, the very near-surface material properties of importance to short-period waves usually are not considered in numerical evaluations of $g(\Delta)$ [such as those of Kanamori and Stewart (1976), from which $g(\Delta)$ in Table 2 was taken]. The additional correction needed to account for propagation from the average crustal depths assumed in evaluating $g(\Delta)$ up to the surface can be approximated by

$$Z(f) = \sqrt{\rho_o c_o / \rho_r c_r}, \quad (3)$$

where the subscripts o and r stand for material properties in average crustal material and near the receiver, respectively (Aki and Richards, 1980, p. 116). A frequency dependence to this correction factor follows by interpreting the receiver properties as being averaged over a depth corresponding to a quarter-wavelength (Joyner and Fumal, 1984). Specific corrections for applications in this paper were obtained by constructing smooth P and S velocity-depth profiles, for rock, constrained by near-

TABLE 2
MODEL PARAMETERS

Parameter	Teleseismic P Waves	Near-Source and Regional S Waves
α	6.8 km/sec	Not needed
β	3.9 km/sec	3.2 km/sec
ρ	3.0 gm/cm ³	2.7 gm/cm ³
$g(\Delta)$	0.32	1.0
F	1.9	2.0
$R_{\Theta\oplus}$	0.45-0.78	0.55
r	6371 km	10 km

surface velocities (Fumal, 1978) and standard crustal velocities. The depth dependence of the velocities are not well determined from the data. They were sketched in, guided by the P_g intercept times of 0.5 to 0.75 sec (J. Eaton and D. Stauber, oral communication, 1984), crack closure experiments of Nur and Simmons (1969), and the frequency dependence of Joyner and Fumal's V_o values. I assumed that standard upper crustal velocities were reached by a depth of 1.5 km. The variations in density are expected to be relatively minor in rock and thus were ignored. The logarithms of the correction factor for several frequencies are given in Table 3. Evaluation at other frequencies was done using linear interpolation.

The diminution function accounts for attenuation of the waves between the source and the receiver. The function combines a near-site attenuation function P , discussed in a later section [equations (13) and (14)], and a standard t^* operator

$$D(f) = \exp[-\pi t^*(f)f]P(f). \quad (4)$$

The frequency dependence of t^* , given by

$$t^* = \begin{cases} a & f \leq 0.13 \text{ Hz} \\ a - 0.27 \log(f/0.13) & f > 0.13 \text{ Hz} \end{cases} \quad (5)$$

where a is an arbitrary constant, approximates that of the preferred QP model of Der and Lees (1985). [Values of A and T calculated from a model with a constant t^* equal to that from equation (5) at a 1.4 sec period differed from results using the frequency-dependent t^* by less than 0.1 log units and 0.14 sec, respectively, for moment magnitudes ranging from 5.0 to 9.5.]

By assuming that the spectral energy given by equation (1) is spread out over a duration τ on the seismogram, random vibration theory (as summarized, e.g., by Boore, 1983) provides a convenient and quick way of estimating the peak motion and the dominant period. The theory uses various weighted integrals of the squared seismograph spectra $R(f)$. These integrals, sometimes referred to as "spectral moments," are defined by the general relation

$$m_k = 2 \int_0^{\infty} (2\pi f)^k |R(f)|^2 df \quad (6)$$

for the k th spectral moment. The simplest random vibration theory uses m_0 and m_2 . For example, from Parseval's theorem, the rms of the seismograph response is

TABLE 3
AMPLIFICATION FACTORS

$\log f$	$\log\sqrt{\alpha_0/\alpha_r}$	$\log\sqrt{\beta_0/\beta_r}$	Gusev (1983)
-1	0.01	0.01	0.0
-0.5	0.04	0.04	0.12
0.0	0.13	0.13	0.25
0.5	0.17	0.34	0.30
1.0	0.19	0.37	0.30

given by

$$r_{rms} = (m_0/\tau)^{1/2}. \quad (7)$$

Less familiar, perhaps, is the following estimate for the dominant period

$$T = 2\pi(m_0/m_2)^{1/2} \quad (8)$$

(e.g., Newland, 1975, pp. 92-94). Once the dominant period and the rms of the motion have been found, random vibration theory can be used to estimate the maximum amplitude in a record of length τ . The simplest expression for doing this is

$$r_{max} \simeq [2 \ln(2\tau/T)]^{1/2} r_{rms}. \quad (9)$$

Equation (9) is an approximation that is good for large values of $2\tau/T$. Although this approximation is adequate for most of the events of interest here, the more exact expressions given by Boore (1983) were used in this paper.

The duration τ was assumed to be related to the inverse of a source corner frequency [for some applications—such as simulations of m_{Lg} —the duration might be controlled by the geologic structure rather than the source (Herrmann, 1985)]. For moderate earthquakes ($M \approx 5$ to 6) with focal depths greater than about 5 to

10 km, the WWSSN short-period instrument response to the direct P wave will not overlap with the response to the depth phases. In this case, the duration τ was taken as the inverse of the source corner frequency, and the radiation coefficient $R_{\Theta\Phi}$ was given by an average of the direct P -wave radiation pattern over all azimuths and over a range of takeoff angles appropriate for the suite of observations (Boore and Boatwright, 1984). For earthquakes greater than about M 8.0 at shallow depths ($h \approx 15$ km), the source duration will be significantly longer than the time interval between the direct- and depth-phase arrivals. To account for the interaction of the various phases, an average radiation coefficient was computed by assuming that the time series of the various phases add incoherently at the frequencies of interest (≈ 1 Hz). Averaging and summing the appropriately weighted radiation patterns for each phase over all azimuths and the appropriate range of takeoff angles led to an effective $R_{\Theta\Phi}$ (Boore and Boatwright, 1984). The effective duration τ was increased by an additive constant equal to a representative time interval between direct and depth phases (7 sec). For this paper, $R_{\Theta\Phi} = 0.45$ for direct P waves and $R_{\Theta\Phi} = 0.78$ for direct P plus pP and sP . These coefficients are appropriate for dipping thrust or normal faults; the coefficients for strike-slip earthquakes would be considerably smaller. The radiation coefficients and the durations for earthquakes with magnitudes between M 6 and M 8 were determined by interpolation.

The random vibration method is a convenient and computationally simple and rapid way of relating time-domain peak motions and spectral-domain amplitudes. For small earthquakes, however, the source process time is comparable to the instrument free-period, and the expected seismograph output has a decidedly nonrandom appearance. It is not clear *a priori* that random vibration theory can be used in such circumstances. The use of random vibration theory was verified, however, for earthquakes down to $M = 5$ by deriving the average A and T from a suite of 25 time-domain simulations for a given moment magnitude, following the methods of Boore (1983).

SCALING RELATIONS FOR SOURCE SPECTRA

For detailed comparison with the data, I have chosen four representative spectral scaling relations, out of the many that have been proposed. Three of the relations are given by models in which the spectral corners scale as $M_0^{-1/3}$ and the high-frequency portions of the spectra are proportional to $\omega^{-1.5}$, $\omega^{-2.0}$, and $\omega^{-3.0}$. The fourth scaling relation is given by the empirical suite of spectra determined by Gusev (1983) in which $S(\omega)$ for large earthquakes has a region of ω^{-1} decay after an initial ω^{-2} falloff. Most attention in this paper will be focused on the Gusev suite of spectra and the source spectra determined from the ω -square model.

The ω -square model used here corresponds to a modification by Joyner (1984) of the models of Aki (1967) and Brune (1970, 1971). Joyner's model allows for the breakdown of the similarity characterizing previous ω -square models; it uses two corner frequencies, the higher frequency one being pinned as the size of the earthquakes passes a specified critical moment magnitude (possibly corresponding to an event that breaks through the seismogenic part of the lithosphere). For events smaller than the critical size, the corners both scale in a self-similar fashion. Because the large earthquakes considered by Houston and Kanamori (1986) correspond to subduction zone events, I have assumed that the critical size earthquake

was never reached. The moment rate function is given by

$$S(f) = \begin{cases} M_0 \left[\frac{1}{1 + (f/f_B)^2} \right]^{1/4} & f \leq f_A \\ M_0 \left[\frac{1}{1 + (f/f_B)^2} \right]^{1/4} \left(\frac{f_A}{f} \right)^{3/2} & f \geq f_A \end{cases} \quad (10a)$$

$$S(f) = \begin{cases} M_0 \left[\frac{1}{1 + (f/f_B)^2} \right]^{1/4} & f \leq f_A \\ M_0 \left[\frac{1}{1 + (f/f_B)^2} \right]^{1/4} \left(\frac{f_A}{f} \right)^{3/2} & f \geq f_A \end{cases} \quad (10b)$$

Following Joyner (1984), f_B was set equal to $4f_A$. This leads to the following expression for f_A

$$f_A = 3.5 \times 10^6 \beta (\Delta\sigma/M_0)^{1/3}, \quad (11)$$

where β is the shear velocity in kilometers/second, $\Delta\sigma$ is a scaling parameter having

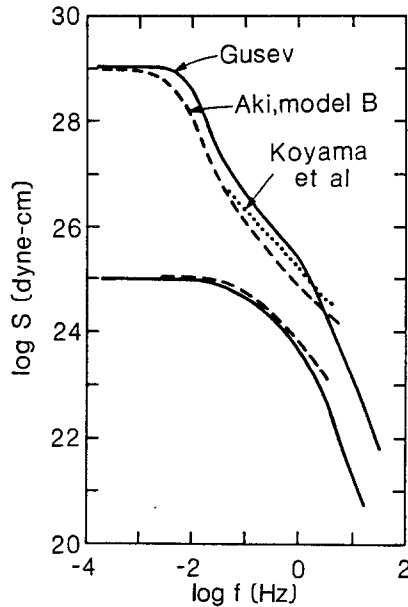


FIG. 3. Source spectra (S) for earthquakes of moment 10^{25} and 10^{29} dyne-cm, modified from Aki (1983). (Solid lines) Gusev (1983); (dashed lines) Aki (1972) model B; (dotted line) Koyama *et al.* (1982).

the dimensions of stress (in units of bars), and the units of moment are dyne-cm. I used equation (11) for *P*-wave spectra, implying no corner frequency shift between *P* and *S* waves. Because the corner frequencies are lower than the instrumental frequency for all but the smallest earthquakes considered here, the effect of a corner frequency shift can be absorbed into a change in $\Delta\sigma$.

The refinements incorporated in Joyner's model are not necessary in this study; simulations with a straightforward, single-corner-frequency ω -square model (such as used in Boore, 1983) generally differed from those predicted by Joyner's model by less than 0.07 log units for log A and 0.1 sec for T . I have kept the Joyner model because it is more flexible and is only slightly more complicated.

Several recent modifications of the ω -square model have introduced a segment of less rapid decay in a portion of the high-frequency part of the spectrum, at least for large events. Figure 3 shows representative spectra from three such studies, by Aki

(1972), Koyama *et al.* (1982), and Gusev (1983). As discussed in some detail later, the main difference between Gusev's spectra and those from the ω -square model arises because of the latter's inability to match the observed M_S , M relation for large earthquakes; Gusev constrained his spectra to do so. Aki (1972) and Koyama *et al.* (1982), on the other hand, modified the ω -square spectra because they thought the ω -square model failed to reproduce the relation between magnitudes determined from surface waves (M_S) and short-period body waves (m_b and M_{JMA} for Aki and Koyama *et al.*, respectively). In Aki's case, the failure to match the $M_S - m_b$ systematics appears to be a consequence of his constraint that $M_S = m_b$ at magnitude 6.75, rather than a fundamental flaw in the model. Although this constraint is a definition used by Gutenberg and Richter in setting up their magnitude scales, it does not apply to modern m_b 's determined from narrow-band, short-period instruments. It is well known that the body-wave magnitudes determined by Gutenberg and Richter (m_B) are measured from broadband instruments and correspond to waves with longer period motions; they are consistently higher than the m_b estimates

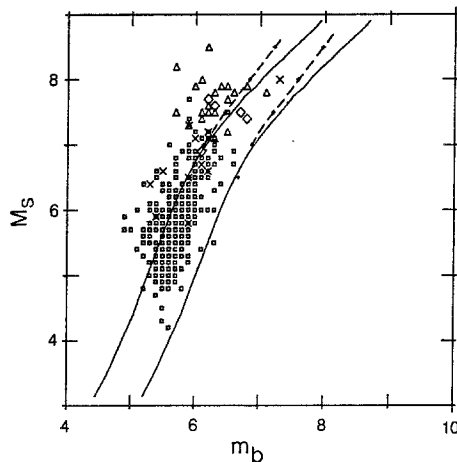


FIG. 4. Correlation of surface-wave magnitude (M_S) and body-wave magnitude (m_b). Data from sources in Figure 1 legend. (Solid lines) Aki's unmodified ω -square model (Aki, 1967), as given in Aki (1972, Figure 8); (dashed lines) include a correction for source duration. (Rightmost lines) Aki's original curves, constrained to pass through the M_S , m_b point (6.75, 6.75); (leftmost curves) the rightmost curves shifted according to Abe's correlation between m_B and m_b (see text).

reported by the NEIS and ISC [Abe (1981), who finds that $m_b = 6.0$ corresponds to the broadband $m_B = 6.75$]. The mismatch of the observations and Aki's original model is illustrated in Figure 4. The right curve is for the ω -square model with and without a correction for source duration, as given in Aki (1972, Figure 8). Clearly, requiring the curve to pass through the point $M_S = m_b = 6.75$ is inappropriate. Shifting the curve to the left by Abe's correction factor of 0.75 results in a good fit to the data, especially if the saturation of m_b is kept in mind (see Figure 1). The modifications of the ω -square model by Koyama *et al.* were similar in spirit to Aki's, but their constraint that the theoretical predictions go through $M_S = M_{JMA} = 7.0$ is consistent with observations. Because a broadband instrument was used, however, I have some reservations about their assumption that M_{JMA} is proportional to the log of the spectral amplitude at a fixed frequency.

Whether or not the modifications to the ω -square are well-founded, the fact remains that a number of recently proposed suites of source spectra exhibit a portion going as approximately ω^{-1} after an initial ω^{-2} decay. I have used Gusev's proposed

spectra for detailed comparisons with data in this paper, and in keeping with the explicit treatment of the wave amplification due to velocity decreases near the earth's surface, I have used his source spectra (which he obtained by deconvolution of the spectra inferred from surface observations) rather than his surface spectra. These spectra, presented only in graphical form, were digitized. Spline interpolations and numerical integration provided the spectral moments needed in the random vibration theory to predict the observational parameters. Comparison of $f^2S(f)$ (proportional to ground acceleration spectra in the absence of attenuation) for Gusev's spectra and those from the ω -square model with a 50 bar stress parameter are shown in Figure 5. The two sets of spectra are similar in the 1 to 10-Hz range for $M_0 > 10^{26}$ dyne-cm but differ radically at longer periods for large earthquakes. Based on this comparison, I would expect that the $M_S - M_0$ relations for the two models would show larger differences than would the predicted peak accelerations and velocities at close distances and $\log A$ values at teleseismic distances. This is indeed the case, as is shown later. In view of the comparison of the two models in Figure 5, it may be more appropriate to say that Gusev's spectra has a "sag" rather than a "bump" (as is commonly done).

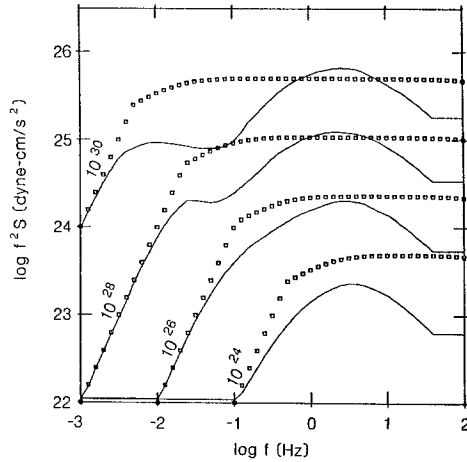


FIG. 5. Source spectra (f^2S) for earthquakes with moments of 10^{24} , 10^{26} , 10^{28} , and 10^{30} dyne-cm. (Lines) Gusev (1983) source spectra; (squares) Joyner (1984), with stress parameter of 50 bars.

Two other models, with high-frequency spectral decays that are more and less rapid than in the ω -square model, were constructed by suitable modification of Joyner's model. In the first, the exponent $3/2$ in equation (10b) was replaced by 1, resulting in a spectral behavior of $\omega^{-1.5}$ at high frequencies. This model was motivated by Hartzell and Heaton's (1985) finding of an average spectral decay of $\omega^{-1.5}$ in the 0.02- to 0.4-Hz frequency band (assuming $t^* = 1.0$) from an analysis of analog records from 63 earthquakes recorded on a single instrument. The second model has a high-frequency behavior of $\omega^{-3.0}$. This ω -cube model was obtained by replacing the exponent $3/2$ equation (10b) by $5/2$. Geller (1976), Evernden (1977), and Frasier and North (1978), among others, have either proposed such ω -cube models or given observational support for an ω^{-3} spectral decay. It is possible to choose values of t^* such that both an ω^{-2} and an ω^{-3} source model will have similar spectral shapes over a limited frequency band, and therefore it is not possible to discriminate between source models on the basis of observed decay alone so long as t^* is a free parameter. For example, Evernden (1977) used an attenuation equivalent to $t^* = 0.26$ in reaching the conclusion that observed spectra agreed with an ω^{-3}

decay. On the other hand, t^* around 0.8 (at the dominant period of the seismogram) seems to be required for the ω^{-2} model. The scaling of $\log A$ with moment is not subject to the same tradeoff between attenuation and spectral decay and therefore should better discriminate between models than does observed spectral shape. This is in essence what Frasier and North (1978) attempted by comparing m_b and dominant period T [their data set, however, was for a small range of m_b ($4 < m_b < 5$) and extrapolation of their m_b , T correlation to larger magnitudes is inconsistent with the data in Figures 1 and 2].

For all the spectral models, the record duration τ for the direct P wave was taken to be $1/f_A$, which is supported by the various estimates of source duration shown in Figure 6. When interpreting this figure, it should be kept in mind that the various authors used different definitions for the duration. Furthermore, the source durations estimated from the moment tensor inversions, as twice the interval between the centroid time and the catalog origin time, could be biased by contributions from

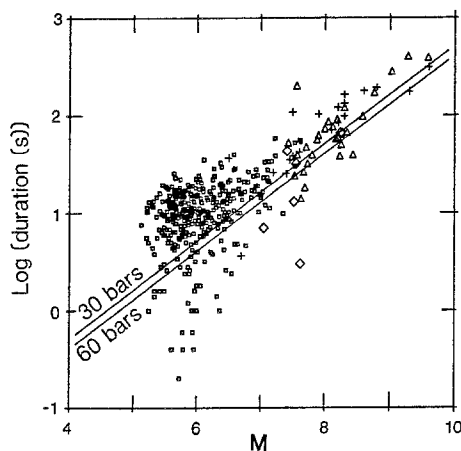


FIG. 6. Estimates of source duration, from references listed in Figure 1 legend. Pluses are $1/2$ the durations reported by Houston and Kanamori (1986). Lines correspond to $1/f_A$ [equation (11)], with $\beta = 3.9$ km/sec and $\Delta\sigma = 30$ and 60 bars (upper and lower lines, respectively).

hypo-center inaccuracies (Giardini, 1984). Included for comparison are the durations computed using equations (11) for $\Delta\sigma = 30$ and 60 bars. In spite of the large scatter, the data seem to agree in slope with the source duration scaling predicted for a constant-stress-parameter model, at least for the larger events. The observed values are underestimated by the model, but this might be a result of the different definitions of duration and at any rate has little effect on the theoretical predictions, which depend on the inverse square root of the duration. With the exception of a smattering of low values of duration, the results of Dzierwonski and colleagues (1983) might be taken to indicate a lower limit of about 10 sec on average for the smaller earthquakes, although the degree to which this conclusion is affected by the previously mentioned qualifications regarding biases in the source time estimates is not known. Calculations show that including a lower limit of 10 sec would reduce the simulated $\log A$ by about 0.2 units for an M 5 event and 0.05 units for an M 7.5 event.

SIMULATION OF A AND T : RESULTS

The simulation techniques and spectral scaling relations were used to make predictions of A and T as a function of moment magnitude at a fixed distance of 70° . The results are given in Figures 7 and 8. Each continuous curve represents the predictions for a given a -value in the equation for frequency-dependent t^* [equation (5)]; for comparison, $a = 0.7, 1.0,$ and 1.3 correspond to $t^* = 0.5, 0.8,$ and 1.1 sec respectively, at a period of 1.4 sec. The predictions were made at half-magnitude

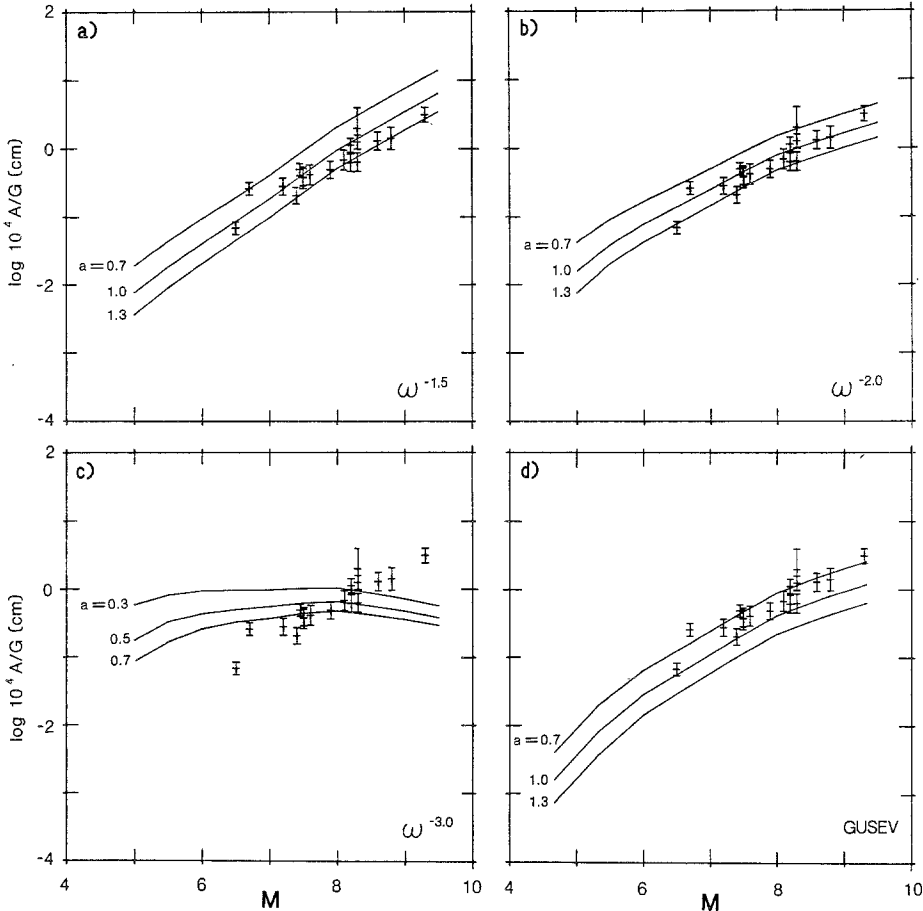


FIG. 7. Observed (symbols) and predicted (lines) amplitudes as a function of moment magnitude. Observations given in Table 1. Predictions for various attenuations [(a) values, see equation (5)] and source spectral models. Stress parameters for (a), (b), and (c) were 5, 50, and 300 bars, respectively.

intervals, thus accounting for some of the lack of smoothness in the curves. The stress parameters given in the figure legends were chosen so as to give a reasonable fit to the observations. It is clear from Figures 7 and 8 that, with the exception of the ω -cube model, the amplitude and period data complement one another— $\log A$ is more sensitive to earthquake size than to attenuation and vice-versa for the period T . Because of its dependence on period, \hat{m}_b shows even less dependence on attenuation than does $\log A$ (this statement is supported by calculations not shown here), thus making it less susceptible to regional variations in attenuation.

The comparison between theory and observation in Figure 7 seems to rule out the ω -cube model, at least if a constant stress parameter is used. This model actually predicts a decreasing $\log A$ with increasing moment magnitude. Hanks (1979) discussed the reasons for this: the high-frequency spectra for the model scale as the stress parameter, which by assumption is constant. In the random model, this constant amount of spectral energy is distributed over an ever increasing time span as the size of the earthquake increases, and therefore the rms (and, as it turns out, the peak) motion decreases with increasing moment magnitude. The obvious way

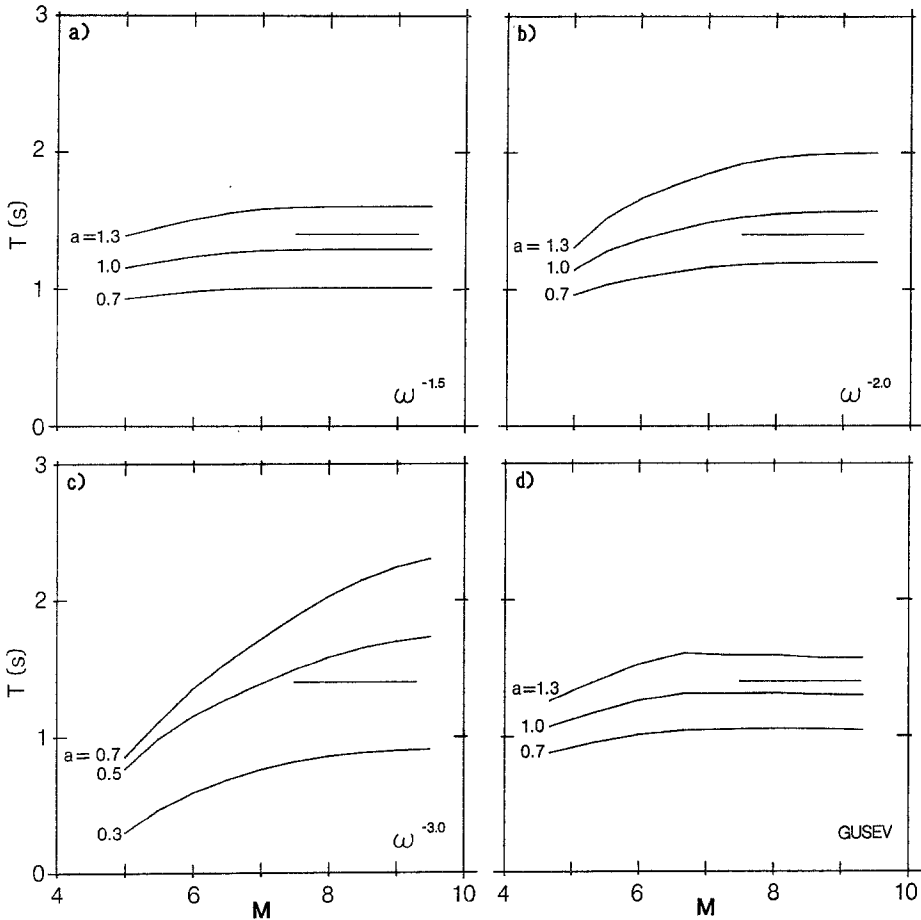


FIG. 8. Observed (short lines) and predicted (long lines) period of P wave on WWSSN short-period instruments estimated from rate of zero crossings. Observed period is an average over a range of moment magnitudes indicated by span of short line (95 per cent confidence limits are ± 0.09 sec). Predictions for various attenuations [(a) values, see equation (5)] and source spectral models. Stress parameters for models in (a), (b), and (c) were 5, 50, and 300 bars, respectively.

to avoid this is to allow an M dependence for $\Delta\sigma$. Such a dependence was devised so as to fit the data qualitatively; the stress parameter for this model ranged from 12 to 1100 bars for earthquakes from M 5 to M 9.5. Of course, allowing $\Delta\sigma$ to depend on moment magnitude would make it possible to fit A perfectly. This would be a highly unlikely model, however, and furthermore would not fit both the peak velocity and peak acceleration data from strong-motion records. It seems reasonable to dismiss the ω -cube model from further consideration in this paper.

The situation is not as clear with the remaining three models. The ω -square model with an a close to 0.9 gives the best simultaneous fit to both $\log A$ and T ; if the observed period of 1.4 sec is taken as a strong constraint (a questionable assumption), a stress parameter of 30 bars gives an even better fit. In either case, the inferred t^* at a 1.4-sec period of about 0.7 is in approximate agreement with that determined by other investigators (Cormier, 1982; Der and Lees, 1985). The $\omega^{-1.5}$ model gives a stronger scaling of $\log A$ with M than does the ω^{-2} model. Although the scatter in the observations makes it difficult to discriminate between lines with different slopes, this stronger scaling does not seem to be supported by the data. This is especially so considering that 5 of the 6 earthquakes with the smallest moments had strike-slip mechanisms, and therefore because of radiation pattern effects, they should have body-wave magnitudes that are systematically lower than other events with comparable moments; this effect would lead to an anomalously steep slope in the data. The calculations based on the Gusev spectra with $a \approx 0.8$ gives a good fit to the $\log A$ observations, but underpredicts the mean of the period observations by about 0.25 sec. As stated, the model using Gusev's spectra has no free parameters (as did the ω -square model) that can be adjusted to improve the fit to both the amplitude and period data. On the other hand, I have assumed that his source spectra can be used to describe *P*-wave radiation, although the spectra were derived from a mixture of *P*- and *S*-wave data. If a shift in the corner frequencies exists, then as pointed out to me by Gusev (written communication, 1985), the *P*-wave radiation may be stronger than assumed in my calculations. As a result, I may be underpredicting the amplitude data.

In summary, in view of the scatter in the data and the simplifications in the models, it is hard to discriminate between the ω -square and Gusev models. The only one that can be clearly eliminated is the constant-stress-parameter ω -cube model. It is of interest to see how the models fare in predictions of peak ground acceleration and velocity at close distances.

PEAK ACCELERATION AND VELOCITY

Accelerograph recordings close to earthquakes provide the most direct measure currently available of the high-frequency radiation from faults. Few such recordings exist, however, for earthquakes greater than about M 7.7, thus providing the motivation for considering short-period *P* waves at teleseismic distances: In an earlier study (Boore, 1983), I compared the available accelerograph data from earthquakes in western North America (with $5.0 \leq M \leq 7.7$) to theoretical predictions from the constant stress parameter, ω -square model in which the energy is distributed randomly over the source duration. The model gave a good fit to many measures of ground motion, including peak acceleration, peak velocity, Wood-Anderson instrument response, and response spectra. I also showed that the peak acceleration and peak velocity data could not both be fit by a stochastic ω -cube model. Although a stress parameter could be found that gave an excellent fit to the peak velocity data, the corresponding predicted peak accelerations underestimated the observations by an amount that increased with moment magnitude (a factor of 2 for $M = 5$ to almost a factor of 5 for $M = 7$).

I have repeated the comparison of theoretical and observed peak accelerations and velocities using the ω -square and Gusev specifications of source spectra. Besides the new spectral scaling, a number of modifications to the model used in Boore (1983) were incorporated in the new calculations. First, explicit account was made

of wave amplification due to decreasing seismic velocities near the Earth's surface (this led to a different $\Delta\sigma$ than found earlier). The amplification factors for shear waves—which dominate horizontal ground motions—are listed in Table 3. Note that they are similar to those used by Gusev (1983). The P - and S -wave amplification factors differ for two reasons: the P - to S -velocity ratio increases near the surface, and for a given frequency the quarter wavelength of a P wave is greater than that of an S wave. The second difference from the earlier model is that a frequency-dependent Q was used in this paper. The specified Q function

$$Q^{-1} = 0.034 \frac{(f/0.3)^2}{1 + (f/0.3)^{2.9}} \quad (12)$$

was based, at high frequencies, on the attenuation of response spectra reported by Joyner and Boore (1982) and at low frequencies follows a general trend governed by the low values of Q^{-1} for surface waves relative to values of Q^{-1} near 1 Hz. A graphical comparison of this function with various measurements compiled by Aki is given in Boore (1984). A third change had to do with the attenuation of high frequencies, irrespective of distance. In Boore (1983), I imposed a high-cut filter with a corner frequency f_m corresponding to the f_{max} of Hanks (1982). This filter had the form

$$P(f) = [1 + (f/f_m)^8]^{-1/2}. \quad (13)$$

It is generally agreed that some form of high-cut filter must be applied to acceleration spectra, at least in standard situations where recordings are made at the Earth's surface. Anderson and Hough (1984) have proposed an alternative form

$$P(f) = \exp(-\pi\kappa f). \quad (14)$$

They found that κ has a small dependence on distance and an intercept of about 0.04 sec on rock at zero distance. Calculations show that the ground motions predicted with the use of equations (13) and (14) are similar if $f_m = 1/\pi\kappa$. I have used both equations (13) and (14) in this paper, with $\kappa = 0.04$ sec in the latter equation. This κ corresponds to $f_m = 8$ Hz, but for consistency with earlier studies, $f_m = 15$ Hz was used in this paper. A few other slight changes relative to the previous study have been made: based on Boore and Boatwright (1984), the average radiation coefficient $R_{\Theta\Phi}$ was reduced to 0.55 from 0.63, and comparisons were made with the expected values of a randomly chosen horizontal component of ground motion rather than the larger of the two horizontal components [according to Joyner and Fumal (1985), this corresponds to a reduction of 0.06 and 0.08 units in the log of peak acceleration and peak velocity, respectively].

Only slight modifications to the theory presented earlier in this paper were necessary for the close-in predictions. In equation (1), r was taken to be the distance from source to receiver, $I(f) = (2\pi f)^n$, where $n = 1$ or 2 for velocity or acceleration, and because the horizontal components, dominated by shear waves, are of most interest, c_s in equation (2) was replaced by β . A multiplicative factor of $1/\sqrt{2}$ was included to account for the partitioning of energy into two horizontal components of motion. The other parameters used are given in Table 2. The calculations were made at a distance of 10 km for the same range of moment magnitudes as used in the simulation of teleseismic observations, although because of geometrical considerations the point source approximation must break down for the larger earthquakes.

The results for peak acceleration and for peak velocity are shown in Figure 9; simulations using the high-cut filter [equation (13)] are given in the left side of the figure and those using Anderson and Hough's filter are given in the right side. The discrepancies between the predictions and the observations are generally less than a factor of 2 (note that the ordinates in Figure 9 cover 3 log units, rather than 6 log units as in Figure 7). As expected, peak acceleration is more sensitive to the high-

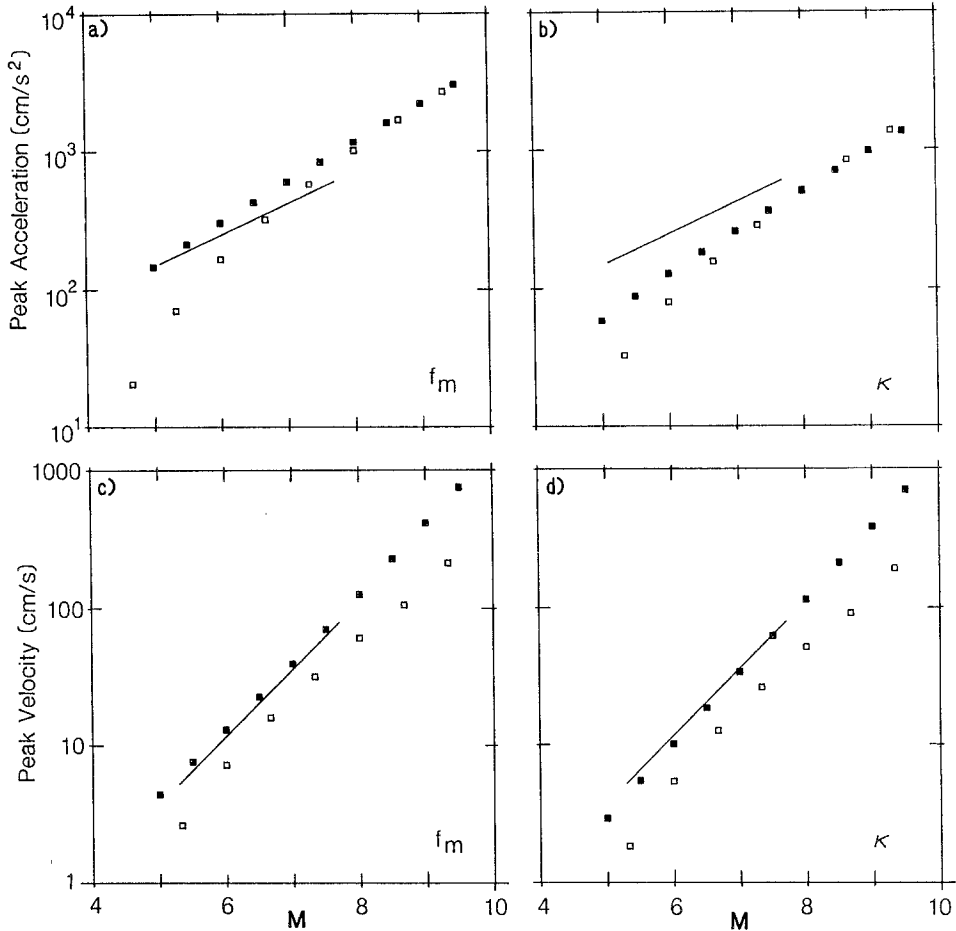


FIG. 9. Peak acceleration and velocity as a function of moment magnitude at a distance of 10 km for average rock site. (Line) Observations summarized by regression analysis of Joyner and Boore (1982), reduced to account for difference between mean of two components and larger of two components (for which regression was calculated). Stated magnitude range of regression's validity indicated by endpoints of line. (Filled squares) Predictions using Joyner (1984) version of ω -square model, with the same stress parameter as in the teleseismic analysis (50 bars); (empty squares) predictions using Gusev's source spectra. High frequencies eliminated using equation (13) with $f_m = 15$ Hz, in *left column*, and equation (14) with $\kappa = 0.04$ sec, in *right column*.

frequency filtering than is peak velocity. The peak acceleration predictions span the estimates based on the regression analyses of data, but this span is due more to the effective cutoff frequencies used in the high-cut filters than it is to the form of the filters. The stress parameter used in the ω -square model is the same as that used in the simulations of A: 50 bars. In my previous study of peak acceleration and velocity, I found that a stress parameter of 100 bars gave a good fit to the data. This apparent inconsistency is a result of my use of an additional amplification

variable in this study. As seen in Table 3, this variable corresponds to a multiplicative factor of about 2.

The model using Gusev's spectra (open squares) gives peak accelerations comparable to the ω -square model (filled squares) for larger earthquakes, as expected from the spectra in Figure 5, and peak velocities lower than those from the ω -square model. According to Gusev (written communication, 1985), the lower values may be due to the high shear velocity ($\beta = 4$ km/sec) he used in reducing the observations to source spectra. It should be noted that I used the P filters [equations (13) and (14)] in computing results for his spectra, although Gusev already accounted for the high-frequency limitation. Computations with and without the P filters, however, showed a maximum difference of only 0.08 units in log acceleration and even a smaller difference in log velocity.

DISCUSSION

Although the comparison of predicted and observed amplitudes and periods on WWSSN short-period seismograms at teleseismic distances and peak accelerations and peak velocities from accelerographs at close distances seems to favor the ω -square spectra over the Gusev (1983) source spectra, the predictions using the two descriptions of source spectra were generally within a factor of 2 of each other—not a large discrepancy by seismological standards. Judging from the spectra in Figure 5, however, the differences would be much larger for predictions of longer period measures (such as M_S) for the larger earthquakes. To utilize this possible discriminant between the two models, a correlation plot of M_S and M for the data appearing in Figure 1 was made, and the predicted dependence of M_S on M for each model was superposed. Unlike A , predictions of M_S were made by assuming that M_S was proportional to the log of spectral amplitudes at a frequency of 0.05 Hz. The resulting curve was constrained to pass through the M_S , M pair (5.85, 6.0)—values determined from a regression analysis by Nuttli (1983a). The resulting comparison (Figure 10) indicates that the Gusev model fits the data well, which it should, because it was constrained to fit a relation between seismic moment and magnitudes based on waves with periods near 20 sec. The ω -square model (not constrained by data at periods near 20 sec) does not fare as well. Although the M_S values of great earthquakes are poorly determined and in fact may represent lower bounds (H. Kanamori, oral communication, 1984), it is unlikely that the discrepancy between the data and the predictions from ω -square spectra can be accounted for by biases in the reported M_S . I did investigate the assumption that M_S is proportional to the log of spectral amplitude, without any regard for source duration. In general, increasing the duration over which spectral energy is distributed will lower the peak motion. If true in the case of M_S , this would lead to lower predicted M_S , and would improve the fit of the ω -square model to the data (and worsen the fit obtained by using Gusev's source spectra). Twenty-five simulated surface wave trains were generated at a fixed distance (70°) for each moment magnitude, using random source phases, the ω -square model, an appropriately chosen excitation function, and dispersion curves for an average structure. Measurements of M_S from these artificial seismograms were averaged and plotted against moment magnitude. When constrained to pass through $M = 6.0$, $M_S = 5.85$, the result was virtually identical to the predicted relation in Figure 10a, thus eliminating one possibility for bringing the M_S prediction from the ω -square model into accord with the observations.

If the observed M_S values for the largest events are biased to the low side, then a model with source spectra intermediate to those given by Gusev and the ω -square model might be justified. A possible model might be constructed by allowing the low-frequency corner (f_A) in Joyner's model to occur at a lower frequency than it now does for the larger earthquakes, followed by a significant interval of decay (in the displacement spectrum) at a less rapid rate than ω^{-2} . In effect, curves for this model would lie between those of ω -square and Gusev in Figure 5, at least up to frequencies around 0.3 Hz. Such a model might be consistent with the decay rates of $\omega^{-1.5}$ and $\omega^{-1.7}$ reported by Hartzell and Heaton (1985).

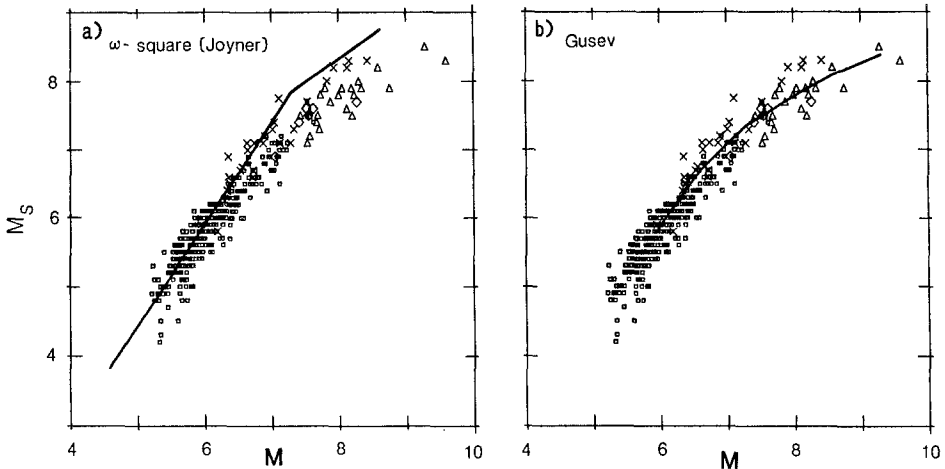


FIG. 10. Correlation of surface-wave magnitude and moment magnitude. (Symbols) Data (see symbols, Figure 1 for reference); (lines) theory, assuming that M_S is proportional to the log of spectral amplitude at a 20-sec period. Lines are constrained to go through the M_S , M point (5.85, 6.0) determined from Nuttli (1983a) regression analysis, using (a) Joyner (1984) source model and (b) Gusev (1983) source spectra.

CONCLUSIONS

As pointed out by Houston and Kanamori (1986), a magnitude measure defined by the largest motion on the direct *P* wave recorded on a WWSSN short-period instrument shows no sign of saturation, even for the largest earthquakes ever recorded. This magnitude and the dominant period on the seismogram provide essential information about the radiation of short-period energy from great earthquakes. Because of a lack of recordings, this information is not available at close and regional distances. The observations were compared to predictions from a simple point-source model that used several different specifications of the source spectra as a function of seismic moment. These spectral scaling laws included modifications of Joyner (1984) in which the stress parameter is constant and the high-frequency spectra are proportional to frequency to the -1.5 , -2.0 , and -3.0 power. Also included were the source spectra derived by Gusev (1983). Of these, the model with a power of -3.0 (the ω -cube model) can be definitely excluded—it completely failed to reproduce the increase of seismogram amplitude with earthquake size. The other three models gave results that were generally similar to one another, with the ω -square model (and a stress parameter of 30 to 50 bars) leading to the best simultaneous fit to the amplitude and period data.

The ability of the models to predict peak acceleration and peak velocity close to faults was also investigated. As shown earlier [McGuire and Hanks (1980), Hanks and McGuire (1981), Boore (1983), Hanks and Boore (1984), McGuire *et al.* (1984), and Atkinson (1984)], the ω -square model is capable of explaining many measures of ground motion, including peak acceleration and velocity. That conclusion was reconfirmed in this study, although inclusion of an explicit correction for amplification of shear waves as they approach the Earth's surface led to a stress parameter half that found in the previous studies. The Gusev model predicted lower peak accelerations and velocities than did the ω -square model, although the two predictions generally differed by less than a factor of two to three.

The stress parameter (50 bars) for the ω -square model turned out to be similar to that found in the study of teleseismic recordings. It is interesting to note that in a previous study (Boore, 1983), 50 bars was also required in fitting peak accelerations and peak velocities from small earthquakes ($0.5 \leq M \leq 2.5$) recorded deep in a South African mine (where the amplification correction was not needed because of the competent nature of the rock). There are enough uncertainties in the model, however, that it is difficult to claim the similarity of the stress estimates as evidence for a universal parameter rather than being a mere coincidence.

The most striking difference between predictions using the Gusev (1983) and ω -square spectra are for M_S values for large earthquakes—the ω -square model predicts much higher values. The predictions using Gusev's spectra fit the observed correlation between M_S and M , which is not a surprise since Gusev constructed his spectra to do so. The failure of the ω -square model near 20-sec period for great earthquakes is of little practical importance. The model works quite well at shorter periods—periods in the range of concern to earthquake engineers.

Although discriminating between various spectral scaling models is of some interest, the most important conclusion of this study may be that a simple source and propagation model, with either ω -square or Gusev spectra, works very well in predicting the high-frequency radiation from moderate to great earthquakes.

ACKNOWLEDGMENTS

Many people contributed to this paper by providing data, encouragement, and criticism. Foremost among them are Heidi Houston and Hiroo Kanamori, who provided data in advance of publication as well as helpful comments at various stages of the work, and Bill Joyner, whose constant enthusiasm and penetrating criticisms were essential to the completion of this study. The technical reviews of these people and also Joe Andrews and Tom Hanks were very useful. A. A. Gusev was kind enough to send me a number of comments on an earlier version of the paper. This work was partially supported by a grant from the U.S. Nuclear Regulatory Commission.

REFERENCES

- Abe, K. (1981). Magnitudes of large shallow earthquakes from 1904 to 1980, *Phys. Earth Planet. Interiors* **27**, 72–92.
- Aki, K. (1967). Scaling law of seismic spectrum, *J. Geophys. Res.* **72**, 1217–1231.
- Aki, K. (1972). Scaling law of earthquake source time-function, *Geophys. J. R. Astr. Soc.* **31**, 3–25.
- Aki, K. (1983). Strong-motion seismology, in *Proceedings of the International School of Physics, Enrico Fermi, Earthquakes: Observation, Theory, and Interpretation*, Varenna, Italy, H. Kanamori and E. Boschi, Editors.
- Aki, K. and P. G. Richards (1980). *Quantitative Seismology*, W. H. Freeman and Co., San Francisco, California.
- Anderson, J. G. and S. E. Hough (1984). A model for the shape of the Fourier amplitude spectrum of acceleration at high frequencies, *Bull. Seism. Soc. Am.* **74**, 1969–1994.
- Atkinson, G. M. (1984). Attenuation of strong ground motion in Canada from a random vibrations approach, *Bull. Seism. Soc. Am.* **74**, 2629–2653.

- Boore, D. M. (1983). Stochastic simulation of high-frequency ground motions based on seismological models of the radiated spectra, *Bull. Seism. Soc. Am.* **73**, 1865–1894.
- Boore, D. M. (1984). Use of seismoscope records to determine M_L and peak velocities, *Bull. Seism. Soc. Am.* **74**, 315–324.
- Boore, D. M. and J. Boatwright (1984). Average body-wave radiation coefficients, *Bull. Seism. Soc. Am.* **74**, 1615–1621.
- Brune, J. N. (1970). Tectonic stress and the spectra of seismic shear waves from earthquakes, *J. Geophys. Res.* **75**, 4997–5009.
- Brune, J. N. (1971). Correction, *J. Geophys. Res.* **76**, 5002.
- Cormier, V. F. (1982). The effect of attenuation on seismic body waves, *Bull. Seism. Soc. Am.* **72**, S169–S200.
- Der, Z. A. and A. C. Lees (1985). Methodologies for estimating $t^*(f)$ from short-period body waves and regional variations of $t^*(f)$ in the United States, *Geophys. J. R. Astr. Soc.* **82**, 125–140.
- Dziewonski, A. M. and J. H. Woodhouse (1983). An experiment in systematic study of global seismicity: centroid-moment tensor solutions for 201 moderate and large earthquakes of 1981, *J. Geophys. Res.* **88**, 3247–3271.
- Dziewonski, A. M., A. Friedman, D. Giardini, and J. H. Woodhouse (1983). Global seismicity of 1982: centroid-moment tensor solutions for 308 earthquakes, *Phys. Earth Planet. Interiors* **33**, 76–90.
- Evernden, J. F. (1977). Spectral characteristics of the P codas of Eurasian earthquakes and explosions, *Bull. Seism. Soc. Am.* **67**, 1153–1171.
- Frasier, C. W. and R. G. North (1978). Evidence for ω -cube scaling from amplitudes and periods of the Rat Island sequence (1965), *Bull. Seism. Soc. Am.* **68**, 265–282.
- Fumal, T. E. (1978). Correlations between seismic wave velocities and physical properties of near-surface geologic materials in the southern San Francisco Bay region, California, *U.S. Geol. Surv., Open-File Rept. 78-1067*, 114 pages.
- Furumoto, M. and I. Nakanishi (1983). Source times and scaling relations of large earthquakes, *J. Geophys. Res.* **88**, 2191–2198.
- Geller, R. J. (1976). Scaling relations for earthquake source parameters and magnitudes, *Bull. Seism. Soc. Am.* **66**, 1501–1521.
- Giardini, D. (1984). Systematic analysis of deep seismicity: 200 centroid-moment tensor solutions for earthquakes between 1977 and 1980, *Geophys. J. R. Astr. Soc.* **77**, 883–914.
- Gusev, A. A. (1983). Descriptive statistical model of earthquake source radiation and its application to an estimation of short-period strong motion, *Geophys. J. R. Astr. Soc.* **74**, 787–808.
- Hanks, T. C. (1979). b values and $\omega^{-\gamma}$ seismic source models: implications for tectonic stress variations along active crustal fault zones and the estimation of high-frequency strong ground motion, *J. Geophys. Res.* **84**, 2235–2242.
- Hanks, T. C. (1982). f_{\max} , *Bull. Seism. Soc. Am.* **72**, 1867–1879.
- Hanks, T. C. and H. Kanamori (1979). A moment-magnitude scale, *J. Geophys. Res.* **84**, 2348–2350.
- Hanks, T. C. and R. K. McGuire (1981). The character of high frequency strong ground motion, *Bull. Seism. Soc. Am.* **71**, 2071–2095.
- Hanks, T. C. and D. M. Boore (1984). Moment-magnitude relations in theory and practice, *J. Geophys. Res.* **89**, 6229–6235.
- Hartzell, S. H. and T. H. Heaton (1985). Teleseismic time functions for large shallow subduction zone earthquakes, *Bull. Seism. Soc. Am.* **75**, 965–1004.
- Herrmann, R. B. (1985). An extension of random vibration theory estimates of strong ground motion to large distances, *Bull. Seism. Soc. Am.* **75**, 1447–1453.
- Houston, H. and H. Kanamori (1986). Source spectra of great earthquakes: teleseismic constraints on rupture process and strong motion, *Bull. Seism. Soc. Am.* **76**, 19–42.
- Joyner, W. B. (1984). A scaling law for the spectra of large earthquakes, *Bull. Seism. Soc. Am.* **74**, 1167–1188.
- Joyner, W. B. and D. M. Boore (1982). Prediction of earthquake response spectra, *U.S. Geol. Surv., Open-File Rept. 82-977*, 16 pp.
- Joyner, W. B. and T. E. Fumal (1984). Use of measured shear-wave velocity for predicting geologic site effects on strong ground motion, *Proc. 8th World Conf. Earthquake Engineering*, San Francisco, California, **II**, 777–783.
- Joyner, W. B. and T. E. Fumal (1985). Predictive mapping of ground motion, in *Evaluating Earthquake Hazards in the Los Angeles Region*, *U.S. Geol. Surv. Profess. Paper 1360*, 203–220.
- Kanamori, H. (1977). The energy release in great earthquakes, *J. Geophys. Res.* **82**, 2981–2987.
- Kanamori, H. and G. S. Stewart (1976). Mode of the strain release along the Gibbs fracture zone, mid-

- Atlantic ridge, *Phys. Earth Planet. Interiors* **11**, 312–332.
- Koyama, J. and S. Zheng (1985). Excitation of short-period body waves by recent great earthquakes, *Phys. Earth Planet. Interiors* **37**, 108–123.
- Koyama, J., M. Takemura, and Z. Suzuki (1982). A scaling model for quantification of earthquakes in and near Japan, *Tectonophysics* **84**, 3–16.
- McGuire, R. K. and T. C. Hanks (1980). rms accelerations and spectral amplitudes of strong ground motion during the San Fernando, California earthquake, *Bull. Seism. Soc. Am.* **70**, 1907–1919.
- McGuire, R. K., A. M. Becker, and N. C. Donovan (1984). Spectral estimates of seismic shear waves, *Bull. Seism. Soc. Am.* **74**, 1427–1440.
- Newland, D. E. (1975). *An Introduction to Random Vibrations and Spectral Analysis*, Longman, London, England.
- Nur, A. and G. Simmons (1969). The effect of saturation on velocity in low porosity rocks, *Earth Planet. Sci. Letters* **7**, 183–193.
- Nuttli, O. W. (1983a). Empirical magnitude and spectral scaling relations for mid-plate and plate-margin earthquakes, *Tectonophysics* **93**, 207–223.
- Nuttli, O. W. (1983b). Average seismic source-parameter relations for mid-plate earthquakes, *Bull. Seism. Soc. Am.* **73**, 519–535.
- Nuttli, O. W. (1985). Average seismic source-parameter relations for plate-margin earthquakes, *Tectonophysics*, **118**, 161–174.
- Richter, C. F. (1958). *Elementary Seismology*, W. H. Freeman and Co., San Francisco, California, 768 pp.
- Silver, P. G. and T. H. Jordan (1983). Total-moment spectra of fourteen large earthquakes, *J. Geophys. Res.* **88**, 3273–3293.
- Willmore, P. L. (Editor) (1979). *Manual of Seismological Observatory Practice*, World Data Center A, Report Series SE-20, U.S. Dept of Commerce, Boulder, Colorado.

U.S. GEOLOGICAL SURVEY
MS 977
345 MIDDLEFIELD ROAD
MENLO PARK, CALIFORNIA 94025

Manuscript received 17 December 1984